Revue des Energies Renouvelables Vol. 13 N°1 (2010) 71 – 84
DOI: https://doi.org/10.54966/jreen.v13i1.179

New method of current control for LCL-interfaced grid-connected three phase voltage source inverter

Nejib Hamrouni*, Moncef Jraidi and Adnane Chérif

Electrical Systems Laboratory, High Engineering Faculty of Tunis
P.B. 37, 1002, Belvedere, Tunis, Tunisia

(reçu le 27 Janvier 2010 – accepté le 28 Mars 2010)

Abstract - *This paper presents an approach for the connection of a photovoltaic generator to the utility grid. A theoretical analysis, modelling, controlling and a simulation of a grid connected photovoltaic system using an output LCL filter are described in detail. In order to reduce the complexity of the system, a linear voltage and current controllers have been developed for a three phase grid connected inverter. Those controllers simultaneously regulate the dc link voltage (the photovoltaic power is delivered to the grid) and the current injected to the grid (to operate at unity power factor). The simulation results show the proposed methods work properly. Moreover they show that the control performance and dynamic behaviour of the inverter-LCL-grid combination. Simulation results show that the output LCL filter installed at the inverter output offer high harmonic attenuation.*

Résumé - *Dans cet article, on s'intéresse à la connexion des générateurs photovoltaïques sur le réseau électrique basse tension. Une étude théorique de modélisation, d'analyse et de contrôle de la connexion du générateur photovoltaïque sur le réseau, moyennant un filtre passif LCL, sera détaillée. En effet, pour réduire la complexité de la commande de système, des régulateurs linéaires seront calculés pour le contrôle du système photovoltaïque en mode connecté. Ces régulateurs permettent simultanément le control de la tension aux bornes du bus continu (pour réaliser le transfert optimal de la puissance photovoltaïque vers le réseau) et du courant injecté par l'onduleur vers le réseau (pour réduire le taux d'harmonique et assurer un facteur de puissance optimal). Les résultats de simulation obtenus, montrent les bonnes performances de la méthode de contrôle calculée. En outre, ils montrent que le filtre, implanté entre l'onduleur et le réseau, permet une bonne atténuation d'harmonique de courant générée par la commande MLI.*

Keywords: LCL filter - Inverter - Grid - Controller - Modelling**.**

1. INTRODUCTION

Renewable energy sources such as solar energy make increasing contributions to electric utility networks. Those sources are commonly coupled to the grid through a pulse width modulation inverter and filter [1]. Different output filter topologies are commonly used to interface inverter to the network, namely the L and the LCL filter. The use of the filter coupling the inverter to the grid reduces the high frequency pollution of the grid that can disturb loads [2].

They provide to the grid a nearly sinusoidal line current waveforms and a low line current distortion [3-5]. Of all filters used in the field of power electronic applications, the LCL filter is currently the most frequently used topologies [6].

* nejib.hamrouni@inrap.rnrt.tn

The inductor L and the capacitor C are locally installed, while the output inductor L includes both locally installed and line inductance. The reason for the popularity of the filter type is that good attenuation is achieved with a relatively small component values. Then, the higher harmonic attenuation permits the use of a lower switching frequency to obtain harmonic limits, increasing efficiency and reasonable costs [7].

This paper presents a modelling and control procedure for a dc link-inverter-LCL filter-utility network combination. PI based controls for the dc voltage and for the ac current have been adopted. The current controllers have been designed in rotating frame [8].

This paper is organized as follows. Section 2 presents a description of the system. Section 3 presents the elementary models of the dc link voltage, the three phase voltage source inverter (VSI) and the output LCL filter. Modelling of the filter was made using the $d-q$ transformation. Section 4 describes the approach of the voltage and the current controllers. Finally, section 5 presents the simulation results.

2. DESCRIPTION OF THE SYSTEM

A three phase voltage source inverter and its controller are shown in Fig. 1. The system is composed of three phase voltage inverter connected to the grid through an output LCL filter.

The input to the inverter is mimicked by a current source which is represented by a photovoltaic generator (PVG) and a $dc-dc$ converter associated with the maximal power point tracking (MPPT) command [9].

Here, the control of $dc-dc$ converter is not covered. The inverter which is the key element of the system is connected to the ac mains through L-C-L combination. Inductor L_2 in Fig. 1 represents the inductance from both the output filter and the distribution line.

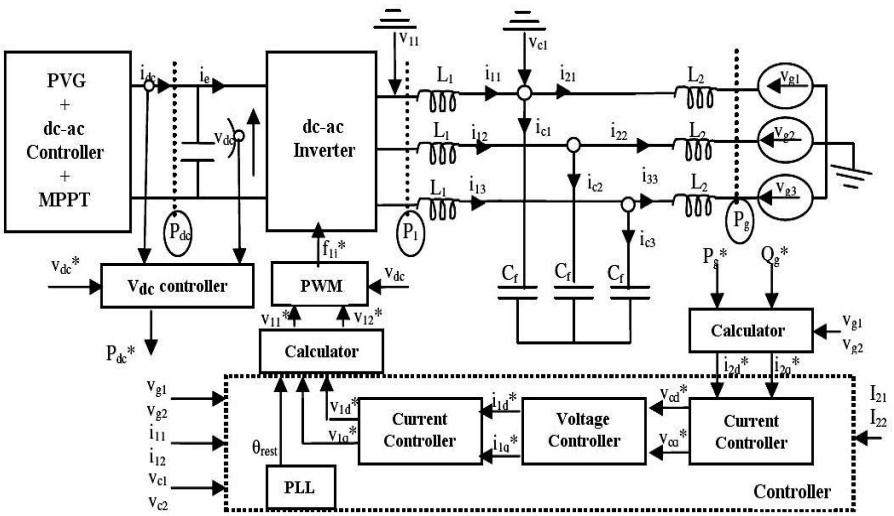

Fig. 1: Block diagram of three phase grid connected inverter and its control

3. MODELLING OF THE SYSTEM

3.1 DC link voltage

Generally, the dc link voltage oscillates between two levels depending on the operating climatic conditions, i.e. ambient temperature and solar radiance. The voltage ripple was minimized by employing relatively large dc link capacitor.

The dc bus voltage is governed by the following equation:

$$\frac{dV_{dc}}{dt} = \frac{1}{C_{dc}}.(i_{dc} - i_e) \tag{1}$$

3.2 Three-phase inverter

An average model for the three phase voltage inverter is presented in [10]. This model describes the relation between dc side and ac side including the connexion functions (f_{11}, f_{12}, f_{13}). This model is adapted to the application studied here. Then, the inverter is considered as a double modulator of variable states. Voltage u_{12} and u_{13} are the modulations of dc link voltage (V_{dc}) and the input inverter current i_e is a modulation of the output currents i_{11} and i_{12}. They can be described as follow [10].

$$\left[i_e\right] = \left[(f_{11} - f_{13}) \quad (f_{12} - f_{13})\right] \times \begin{bmatrix} i_{11} \\ i_{12} \end{bmatrix} \tag{2}$$

$$\begin{pmatrix} u_{12} \\ u_{13} \end{pmatrix} = \begin{pmatrix} \dfrac{f_{11} - f_{13}}{f_{12} - f_{13}} \end{pmatrix} \times v_{dc} \tag{3}$$

f_{11}, f_{12}, f_{13} are the connection functions between the dc side and ac side variables. They have a binary value (0, 1).

3.3 Output LCL filter

Assuming that the impedance of the three phase system corresponding to figure are balanced, the equations governing the three phase voltage and current are:

$$L_1 \frac{di_{1j}}{dt} = v_{cj} - R_1 i_{1j} - v_{1j} \tag{4}$$

$$C_f \frac{dv_{cj}}{dt} = i_{1j} - i_{2j} \tag{5}$$

$$L_2 \frac{di_{2j}}{dt} = v_{2j} - R_2 i_{2j} - v_{cj} \tag{6}$$

where: j is the phase number equal to {1, 2 and 3}.

The three phase vectors in (4), (5) and (6) can be replaced by complex vectors by applying the amplitude invariant Clarke transformation and assuming no zero sequence.

$$\begin{pmatrix} x_\alpha \\ x_\beta \\ x_0 \end{pmatrix} = \frac{2}{3}\begin{pmatrix} 1 & -\frac{1}{2} & -\frac{1}{2} \\ 0 & \frac{\sqrt{3}}{2} & \frac{\sqrt{3}}{2} \\ \frac{1}{\sqrt{2}} & \frac{1}{\sqrt{2}} & \frac{1}{\sqrt{2}} \end{pmatrix} \times \begin{pmatrix} x_1 \\ x_2 \\ x_3 \end{pmatrix} \tag{7}$$

Thus, the differential equations of LCL filter in the stationary reference $\alpha-\beta$ frame are:

$$\frac{d}{dt}\begin{pmatrix} i_{1\alpha\beta} \\ v_{c\alpha\beta} \\ i_{2\alpha\beta} \end{pmatrix} = \begin{pmatrix} -\frac{R_1}{L_1} & -\frac{1}{L_1} & 0 \\ \frac{1}{C_f} & 0 & -\frac{1}{C_f} \\ 0 & \frac{1}{L_2} & -\frac{R_2}{L_1} \end{pmatrix} \times \begin{pmatrix} i_{1\alpha\beta} \\ v_{c\alpha\beta} \\ i_{2\alpha\beta} \end{pmatrix} + \begin{pmatrix} \frac{1}{L_1} & 0 \\ 0 & 0 \\ 0 & -\frac{1}{L_2} \end{pmatrix} \times \begin{pmatrix} V_{inv\alpha\beta} \\ V_{g\alpha\beta} \end{pmatrix} \tag{8}$$

Let's consider the model developed in a general frame that rotates at w angular speed. In that frame six equations can be written according to (9-14).

Transformation of the state description in stationary coordinate $\alpha-\beta$ into the synchronously rotating reference $d-q$ frame is obtained by subtraction of the angle difference as described in figure 2.

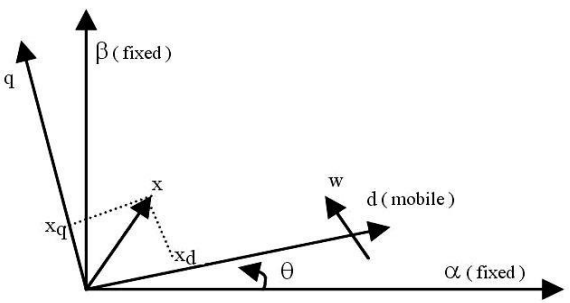

Fig. 2: Relationship between $\alpha-\beta$ and $d-q$ frame

The real valued state space description of the output LCL filter model is obtained by separating the vector equations in their real and imaginary parts. Assuming R_1 and R_2 are different to zero, the complex $d-q$ frame differential equations are then given by:

$$\frac{di_{1d}}{dt} = -\frac{R_1}{L_1} i_{1d} + w\, i_{1q} + \frac{1}{L_1} v_{1d} - \frac{1}{L_1} v_{cd} \tag{9}$$

$$\frac{di_{1q}}{dt} = -\frac{R_1}{L_1} i_{1q} - w\, i_{1d} + \frac{1}{L_1} v_{1q} - \frac{1}{L_1} v_{cd} \tag{10}$$

$$\frac{dv_{cd}}{dt} = w v_{cq} + \frac{1}{C_f} i_{1d} - \frac{1}{C_f} i_{cd} \tag{11}$$

$$\frac{dv_{cq}}{dt} = -w v_{cq} + \frac{1}{C_f} i_{1q} - \frac{1}{C_f} i_{cq} \tag{12}$$

$$\frac{di_{2d}}{dt} = -\frac{R_2}{L_2} i_{2d} + w i_{2q} + \frac{1}{L_2} v_{gd} - \frac{1}{L_2} v_{cd} \tag{13}$$

$$\frac{di_{2q}}{dt} = -\frac{R_2}{L_2} i_{2q} - w i_{2d} + \frac{1}{L_2} v_{gq} - \frac{1}{L_2} v_{cq} \tag{14}$$

The complex valued state description in $d-q$ frame indicates that the behaviour of the output LCL filter is dependent on the rotation direction of the vectors.

There are three reactive elements L_1, C_f and L_2, and this yields a third order system. The inputs are the inverter voltage (V_{1dq}) and the grid voltage (V_{gdq}). The state and the output variables of the system are the currents through L_1 (i_{1dq}) and L_2 (i_{2dq}) as well as the capacitor voltage (v_{cdq}).

4. CONTROL OF THE SYSTEM

The overall control structure consists of a DC link voltage controller and a line current controller, refer to figure 1. To supply a line current with low distortion the connection to the grid is made via an ac filter witch consists of L-C-L combination. The line current controller consists of a model based cascade controller.

The cascade controller is composed of an outer current controller for the network line current, i.e. current i_{2j}, an intermediate voltage controller for the filter capacitor voltage and an inner current control loop for the inverter current i_{1j}. The cascade configuration enables the use of proportional or proportional-integral controllers.

4.1 DC link voltage control

The purpose of the DC link voltage controller is to preserve the DC-link voltage at its reference value ($v_{dc}*$) and to provide the reference current (i_e*). This controller achieved the transfer of the active power flow, drawn from the photovoltaic generator, to the utility network.

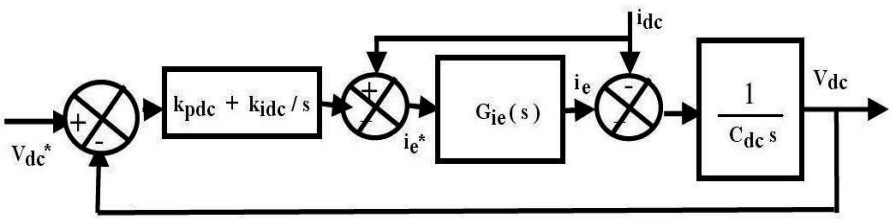

Fig. 3: DC-link voltage regulator

The block diagram representation of the DC-link voltage control loop is shown in Fig. 3. The DC-link voltage controller is designed in the continuous time domain. It consists of P-I controller where the integral part reduces the steady state error of the DC- link voltage.

The dc bus transfer function in the continuous time domain is as follow:

$$G_{dc}(s) = \frac{1}{s.C_{dc}} \tag{15}$$

The transfer function of the P-I controller is given by:

$$P.I = k_{pdc} + \frac{k_{idc}}{s} \tag{16}$$

where, k_{pdc} and k_{idc} are respectively proportional and integral gains. The current sourced into the dc bus is denoted by i_{dc}. The dc bus capacitance is denoted by C_{dc}.

We can equalize the transfer function between the current i_e and its reference to a first order function.

$$G_{ie}(s) = \frac{1}{\tau_{ri}.s + 1} \tag{17}$$

In general the current tuning dynamics is very higher than the voltage, so it is possible to consider it as infinite for the synthesis of the corrector. The input reference active power injected to the electrical supply network is given by:

$$P_{dc}^* = i_i^* \times V_{dc} \tag{18}$$

The active power injected to the grid is

$$P_g^* = P_{dc}^* - \sum(P_{dc-ac}, P_{LCL}) \tag{19}$$

where, P_{dc-ac} is the loss power which due to the conduction and commutation of the IGBT, whereas P_{LCL} is the instantaneous power absorbed by the filter resistors.

To achieve steady state operation the supplied dc power of the PVG and the ac power fed into the grid must be balanced. The dc voltage controller gives the set point of the ac power. Assuming, in this paper, that there is no power losses in the inverter and the LCL filter. Then, we can consider:

$$P_g^* \approx P_{dc}^* \tag{20}$$

If only active power is to be injected in the grid:

$$Q_g = 0 \tag{21}$$

Network reference currents, expressed in $d-q$ frame, are given by the following relation [10]:

$$\begin{bmatrix} i_{2d}^* \\ i_{2q}^* \end{bmatrix} = \frac{1}{V_{gq}^2 + V_{gd}^2} \times \begin{bmatrix} P_g^* & -Q_g^* \\ Q_g^* & P_g^* \end{bmatrix} \times \begin{bmatrix} V_{gd} \\ V_{gq} \end{bmatrix} \tag{22}$$

4.2 Grid side current Controller

Fig. 4 shows the grid side current controller block diagram including all feed back and feed forward terms. The input of the current controller is split into two terms; the reference input (i_{2dq}^*) and the feedback input (i_{2dq}). Output current inverter is achieved with standard P-I controllers. The corresponding state equations are [8]:

$$\Delta i_{2d} = i_{2d}^* - i_{2d} \tag{23}$$

$$\Delta i_{2q} = i_{2q}^* - i_{2q} \tag{24}$$

The complex $d-q$ frame differential equations (13) and (14) became:

$$L_2 \frac{d}{dt}(i_{2d}^*) + R_2 i_{2d} - \omega L_2 i_{2q} + v_{gd} - v_{cd} = L_2 \frac{d}{dt}(\Delta i_{2d}) \tag{25}$$

$$L_2 \frac{d}{dt}(i_{2q}^*) + R_2 i_{2q} + \omega L_2 i_{2d} + v_{gq} - v_{cq} = L_2 \frac{d}{dt}(\Delta i_{2qd}) \tag{26}$$

where

$$v_{cd}^* = L_2 \frac{d}{dt}(i_{2d}^*) + R_2 i_{2d} - \omega L_2 i_{2q} + v_{gd} \tag{27}$$

$$v_{cq}^* = L_2 \frac{d}{dt}(i_{2q}^*) + R_2 i_{2q} + \omega L_2 i_{2d} + v_{gq} \tag{28}$$

The variation between the reference voltage v_{cdq}^* and the measured v_{cdq} produces an error on the current injected into the network. According to (27) and (28), the voltage v_{cdq}^* is composed of two terms.

The first term represents the network voltage v_{gdq} which is directly measurable, whereas the second term represents the voltage drop of the equivalent impedance when it is crossed by a current i_{2dq}.

According to [11], terms (27) and (28) must be elaborated by current controllers given by Fig. 4.

4.3 Voltage controller

Fig. 5 shows the voltage controller bloc diagram. It includes feed back and feed forward terms. The capacitor voltage control is makes with a P-I controller. The corresponding state equations are:

$$\Delta v_{cd}^* = v_{cd}^* - v_{cd} \tag{29}$$

$$\Delta v_{cq}^* = v_{cq}^* - v_{cq} \tag{30}$$

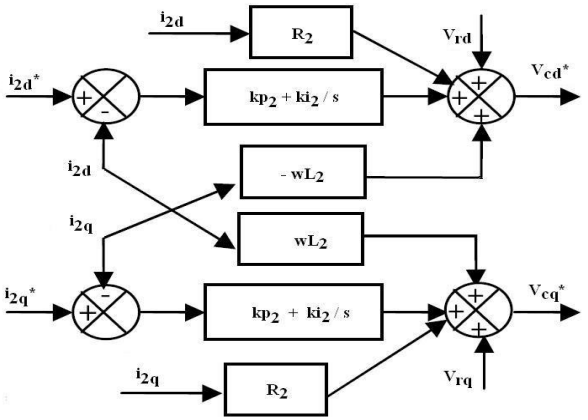

Fig. 4: Grid side current controller

The complex $d-q$ frame differential equation (11) and (12) became:

$$C_f \frac{d v_{cd}^*}{dt} - C_f \omega v_{cq} + i_{2d} - i_{1d} = C_f \frac{d}{dt}(\Delta v_{cd}) \tag{31}$$

$$C_f \frac{d v_{cq}^*}{dt} + C_f \omega v_{cd} + i_{2q} - i_{1q} = C_f \frac{d}{dt}(\Delta v_{cq}) \tag{32}$$

where:

$$i_{1d}^* = C_f \frac{d v_{cd}^*}{dt} - C_f \omega v_{cq} + i_{2d} \tag{33}$$

$$i_{1q}^* = C_f \frac{d v_{cq}^*}{dt} + C_f \omega v_{cd} + i_{2q} \tag{34}$$

The variation between the reference voltage i_{1dq}^* and the measured i_{1dq} produces an error on the capacitor voltage. According to the (33) and (34), the current i_{1dq}^* is composed of two terms.

The first term represents the network current i_{1dq} which is directly measurable, whereas the second term represents the current crossed the capacitor when it is feed by a voltage v_{cdq}. Terms (33) and (34) must be elaborated by voltage controllers shown in Fig. 5.

4.4 Inverter Side Current controller

The side inverter current controller is shown by figure 1. Inductor current controller is achieved with a P-I corrector. The corresponding state equations are:

$$\Delta i_{1d} = i_{1d}^* - i_{1d} \tag{35}$$

$$\Delta i_{1q} = i_{1q}^* - i_{1q} \tag{36}$$

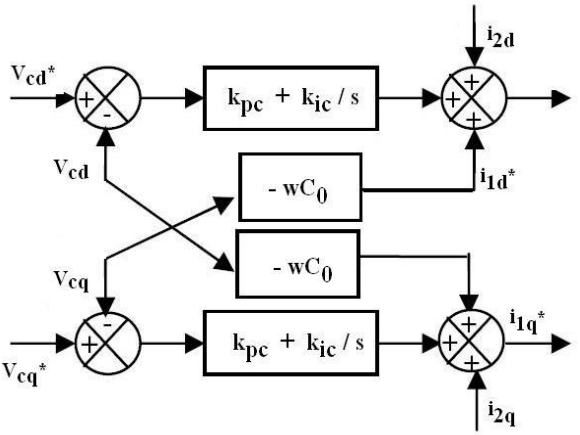

Fig. 5: Voltage controller

The complex $d-q$ frame differential equations (9) and (10) became:

$$L_1 \frac{d}{dt}(i_{1d}^*) + R_1 i_{1d} - \omega L_1 i_{1q} + v_{cd} - v_{1d} = L_1 \frac{d}{dt}(\Delta i_{1d}) \tag{37}$$

$$L_1 \frac{d}{dt}(i_{1q}^*) + R_1 i_{2q} + \omega L_1 i_{Id} + v_{cq} - v_{1q} = L_1 \frac{d}{dt}(\Delta i_{1q}) \tag{38}$$

where:

$$v_{1d}^* = L_1 \frac{d}{dt}(i_{1d}^*) + R_1 i_{1d} - \omega L_1 i_{1q} + v_{cd} \tag{39}$$

$$v_{1q}^* = L_1 \frac{d}{dt}(i_{1q}^*) + R_1 i_{1q} + \omega L_1 i_{1d} + v_{cq} \tag{40}$$

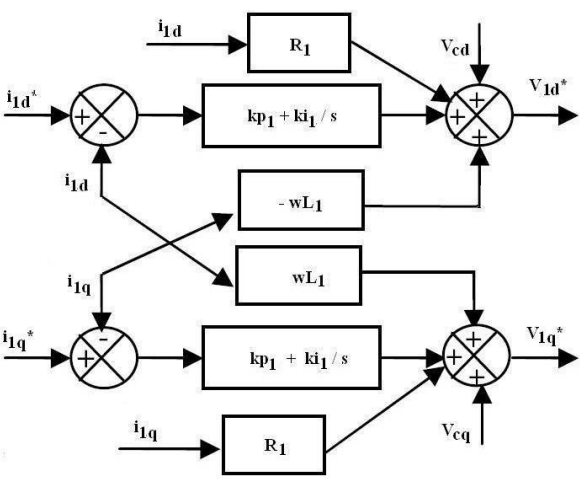

Fig. 6: Inverter side current controller

The variation between the reference voltage v_{1dq}* and the measured v_{1dq} produces an error on the current supplied by the inverter. According to (40) and (41), the voltage v_{1dq} is composed of two terms. T

he first term represents the capacitor voltage v_{cdq} which is directly measurable, whereas the second term represents the voltage drop of the filter impedance when it is crossed by a current i_{1dq}. Terms (40) and (41) must be elaborated by current controllers according to Fig. 6.

5. SIMULATION OF THE SYSTEM

The rated RMS voltage is 380 V and the rated power of the PVG is about 2,5 kWp (calculated in standard climatic conditions: 1000 W/m^2 and 25 °C). The modulation strategy adopted is the symmetrical PWM. The DC voltage reference is 550 V.

The salient parameters for the system are shown in **Table 1**. The controller parameters (**Table 2**) were chosen to minimize both the time response and the steady state error and to maintain the stability of the system.

Fig. 7 shows the measured and reference capacitor voltages in the rotating reference frame. Both d and q capacitor voltage are closely regulated through the action of the voltage control loops.

The inverter and grid currents obtained with LCL filter, at rated condition in simulation are reported in Fig. 8. The q axis currents i_{1q} and i_{2q} follow their respective deadbeat references i_{1q}* and i_{2q}*.

Fig. 9 shows the output inverter current. There is a big harmonic around the switching frequency on the inverter side is $2A_{rms}$.

Table 1: System parameters

Parameter	C_{pv}	L_{pv}	R_{pv}	C_{dc}	L_1	R_1	C_f	L_2	R_2
Value	5mF	24.9mH	0.5Ω	9mF	19mH	0.5Ω	10µF	20mH	0.5Ω

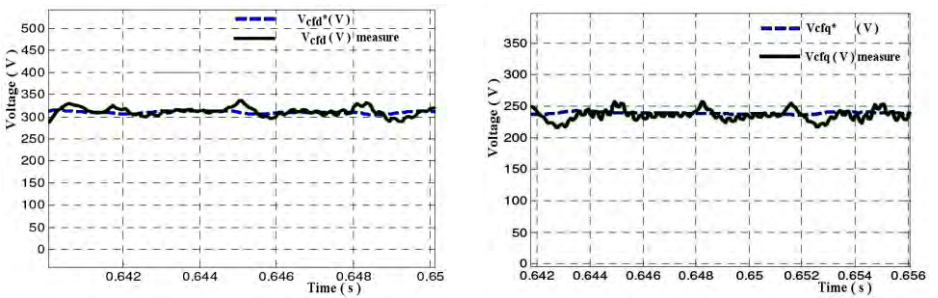

Fig. 7: d components and q components of the capacitor voltages of the filter LCL (measures and references)

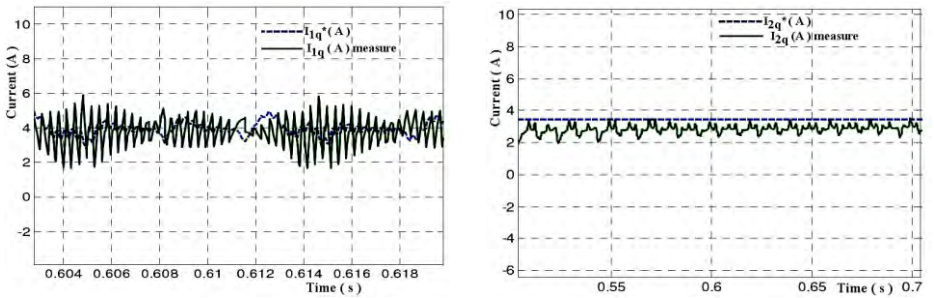

Fig. 8: q components of the output currents of the inverter and the LCL filter (measures and references)

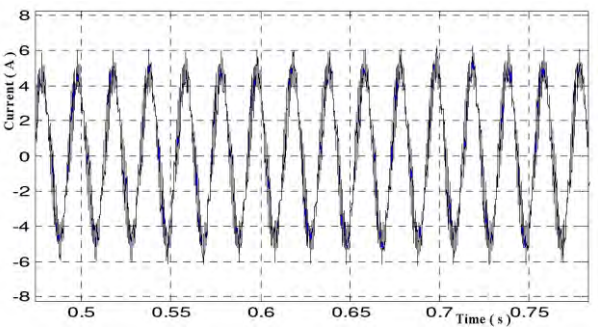

Fig. 9: Output current of the inverter

Fig. 10 presents the dc side voltage. It can be seen that the dc measured voltage follow instantaneously its deadbeat references voltage v_{dc}*. In steady state the dc bus voltage is stabilized at 549 V with an error equal to 0.1 %. Fig. 11 and 12 present respectively the active and reactive power fed into the grid, when the PVG is delivering 2600 W.

The oscillation in the power waveforms is due to the existence of some harmonics in output line current supplied by the LCL filter. Then design of the LCL filter must be investigated.

Fig. 13 shows the dc side voltage and current with the input voltage v_g = 220 V.

As it might be noticed in this figure, there isn't a phase leading/lagging between grid side line current and voltage. They are in phase and sinusoidal. As a result, a unit power factor is achieved. The THD of the current is very low (< 2 %).

Table 2: System parameters

Parameter	k_{i2}	k_{p2}	k_{ic}	k_{pc}	k_{il}	k_{pl}	k_{idc}	k_{pdc}
Value	0.003	10	0.002	0.05	0.002	50	0.001	0.0001

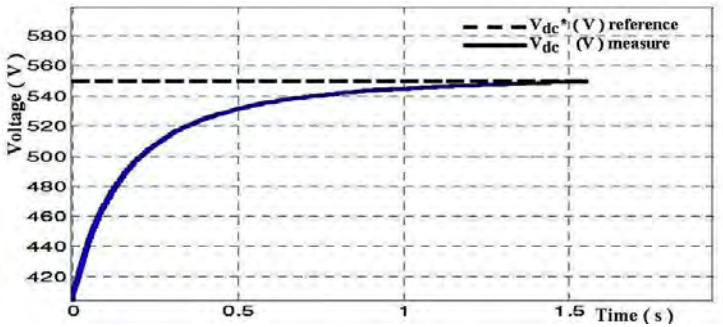

Fig. 10: DC link voltage (measure and reference)

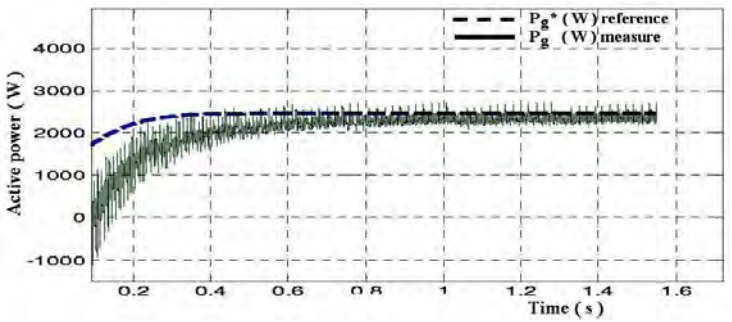

Fig. 11: Active power injected to the grid (measure and reference)

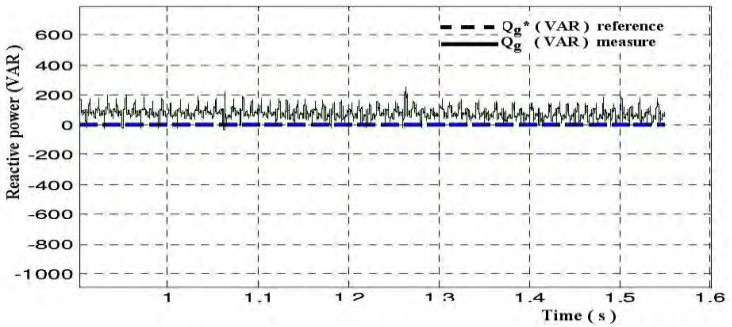

Fig. 12: Reactive power injected to the grid (measure and reference)

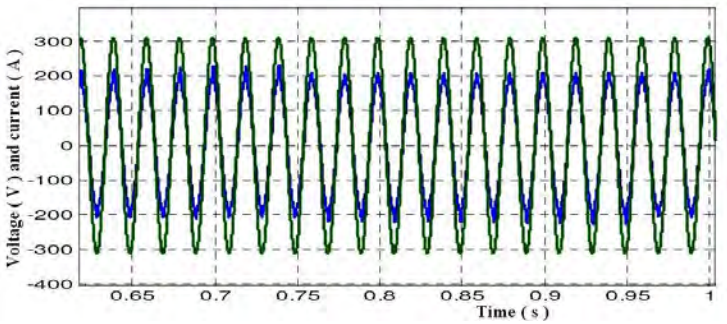

Fig. 13: Phase-voltage and (.*50) phase-current of the grid

6. CONCLUSION

In the paper both the modelling and control of a three phase inverter employing an LCL filter used to reduce the switching frequency ripple injected to the grid is investigated.

The goal of the paper is to provide a control procedure for the inverter-LCL-grid combination and study the performance and the dynamic of linear controllers calculated to control the dc link voltage and the output inverter current.

The modelling and control have been tested with simulation. Stability and high dynamic are obtained, and moreover all results have been obtained using a simple control method but more sensors.

NOMENCLATURE

VSI : Voltage source inverter

$MLI'PWM'$: Pulse width modulation

$MPPT$: Maximal point tracking power

Q_g : Reactive power injected to the grid (VAR)

Δv : Variation between the reference and the measured voltage (V)

f_{11}, f_{12}, f_{13} : Connections functions

u_1, u_2 : Inverter output voltage (A)

τ_{ri} : Time constant of the dc link voltage regulator

i_{11}, i_{12} : Inverter output current (A)

L_1 : Inductor side the grid (H)

R_1 : resistor of the inductor side the grid (Ω)

L_2 : Inductor side the inverter (H)

$R2$: resistor of the inductor side the inverter (Ω)

C_f : Capacitor of the filter (F)

C_{dc} : Capacitor of the dc link voltage (F)

P_{dc-ac} : Loss power which due to the conduction and commutation of the IGBT (W)

P_{LCL} : Instantaneous power absorbed by the filter resistor (W)

P_g : Active power injected to the grid (W)

i_e : Inverter input current (A)

v_{gq}, v_{g_q} : Components of the grid voltage in dq frame (V)

Δi : Variation between the reference and the measured current (A)

PVG : Photovoltaic generator

V_{dc} : DC link voltage (V)

k_{pdc} : Gain of the dc link voltage regulator

k_{idc} : Integral part of the dc link voltage regulator

k_{pc} : Gain of the capacitor voltage regulator

k_{ic} : Integral part of the capacitor voltage capacitor

k_{pl} : Gain of the current regulator side the inverter

k_{il} : Integral part of the current side the inverter

k_{p2} : Gain of the current regulator side the grid

k_{i2} : Integral part of the current regulator side the grid

ω : Pulsation of the grid voltage (rd/s)

REFERENCES

[1] M. Liserre, F. Blaabjerg and S. Hansen, '*Design and Control of an LCL-Filter Based Three Phase Active Rectifier*', Industry Applications Conference, 36 IAS Annual Meeting, 30 Sep - 4 Oct 2001, Conference record of IEEE, Vol. 1, pp. 299 - 307, 2001.

[2] W.A. Hill and S.C. Kapoor, '*Effect of Two Level PWM Sources on Plant Power System Harmonics*', Proceedings IAS Conference, Vol. 2, pp. 1300 - 1306, S^{t} Louis, USA, October 1998.

[3] S. Hansen, M. Malinowski, F. Blaabjerb and M.P. Karmierkowski, '*Sensorless Control Strategies for PWM Rectifiers*', Proceedings of APEC Conference, New Orleans (USA), February 2000.

[4] M. Malinowski, M.P. Karmierkowski, S. Hansen, F. Blaabjerb and G Marques, '*Virtual Flux Based Direct Power Control of Three Phase PWM Rectifiers*', In IEEE Transactions on Industrial Applications, Vol. 37, pp. 1019 – 1027, July/August 2001.

[5] A. Dell'Aquilla, L. Coponio, M. Liserre, C. Cecati and A. Ometto, '*A Fuzzy Logic Feed-Forward Current Controller for PWM Rectifiers*', In Proceedings of IEEE ISIE 2000, Puebla, Mexico, pp. 430 – 435, December 2000.

[6] T.C.Y. Wang, Z. Ye, G. Sinha and X. Yuan, '*Output Filter Design for a Grid Interconnected Three Phase Inverter*', Power Electronics Specialist Conference, PESC'03. IEEE 34th Annual, Vol. 2, pp. 779 - 784. June 2003.

[7] M. Lindgreen and J. Svenson, '*Connecting Fast Switching Voltage Source Converters to the Grid Harmonic Distortion and Its Reduction*', in IEEE/ Stokholm Power Tech. Conference, Stockholm, Sweden, June 18 – 22, 1995. Proceedings of Power Electronics, pp. 191 – 195, 1995.

[8] N. Pogaku, M. Prodanovic and T.C. Green, '*Modelling, Analysis and Testing of Autonomous Operation of an Inverter-Based Microgrid*', IEEE Transactions on Power Electronics, Vol. 22, N°2, pp. 613-625, March 2007.

[9] Y. Pankow, '*Etude de l'Intégration de la Production Décentralisée dans les Réseaux Basse Tension. Application au Générateur Photovoltaïque*', Thèse de Doctorat, ENSAM, Lille, France, 2005.

[10] B. François, '*Conception des Dispositifs de Commandes des Convertisseurs de Puissance par Modulation Directe des Conversions. Perspectives pour l'Insertion de Production d'Energie Dispersée dans les Réseaux Electriques*', Habilitation à Diriger des recherches, UST-Lille 2003

[11] M.A.E. Alali, '*Contribution à l'étude des Compensateurs Actifs des Réseaux Electriques Basse Tension*', Thèse de Doctorat, Université Louis Pasteur, Strasbourg, France, 2002.